

Kinetic Analysis of the Stepwise Platination of Single- and Double-Stranded GG Oligonucleotides with Cisplatin and *cis*-[PtCl(H₂O)(NH₃)₂]⁺

Susan J. Berners-Price, Kevin J. Barnham, Urban Frey and Peter J. Sadler*

Abstract: We report the first direct comparison of the kinetics of platination of defined single- and double-stranded DNA with the anticancer drug cisplatin. The courses of the reactions of the 14-mer duplex d(A-T-A-C-A-T-G-G-T-A-C-A-T-

with [¹⁵N]cisplatin and *cis*-[PtCl(H₂O)-(¹⁵NH₃)₂]⁺ and of each of the single strands with [¹⁵N]cisplatin have been studied at 298 K, pH 6, by [¹H,¹⁵N] NMR spectroscopy. As expected the reactions of cisplatin proceed via *cis*-[PtCl(H₂O)(NH₃)₂]⁺, and lead to two monofunctional adducts on the duplex and two

on the GG single strand. In both the GG single strand and the duplex, one of the two G's is platinated faster than the other (by a factor of ca. 4). Remarkably, ring closure on the duplex to form the GG chelate occurs about an order of magnitude faster for one monofunctional adduct than for the other. The latter mono-

functional adduct has distinctive ¹H and ¹⁵N NMR chemical shifts for Pt-NH₃, and is very long-lived (persists for > 5 d). The Pt-Cl bond in this monofunctional adduct is protected from hydrolysis by the duplex. In contrast, the two monofunctional adducts on the GG single strand undergo ring closure at about the same rate. Equilibria between kinked and distorted forms of the GG platinated duplex, the platination of G's on the complementary strand, and the potential biological significance of long-lived monofunctional adducts of platinum drugs with DNA are discussed.

Keywords

antitumour agents · DNA · kinetics · nucleotides · platinum complexes

Introduction

The antitumour activity of the anticancer drug cisplatin, *cis*-[PtCl₂(NH₃)₂], depends on its ability to modify the structure of the DNA of cancer cells in such a way that enzymatic excision repair is avoided. The most electron-donating sites on duplex DNA are known to be guanine residues located adjacent to a second guanine residue,^[1, 2] and it is therefore perhaps not surprising that the major DNA lesions are intrastrand d(GpG) crosslinks which unwind and bend the duplex. These are shielded from repair by high mobility group proteins which recognize them.^[3] Besides GG intrastrand crosslinks (70%), the other major Pt-DNA adducts are intrastrand AG (but not GA) crosslinks (15%), the remainder being minor 1,3-intrastrand and interstrand crosslinks.^[4]

The conformational changes that accompany the formation of intrastrand d(GpG) crosslinks on single-stranded and duplex DNA have been elucidated both in solution and in the solid, crystalline state. Early studies^[5, 6] of

d(TCTCG*G*TCTC)·d(AGAGCCAGAG) (where * denotes the site of [Pt(NH₃)₂]²⁺ chelation through N7) in solution showed that hydrogen bonding can be maintained in a duplex after platination, but that vertical stacking interactions between bases are distorted. In a recent X-ray crystal structure^[7] of d(CCU^BCTG*G*TCTCC)·(GGAGACCAGAG), the duplex is bent towards the major groove without disrupting the normal Watson-Crick base-pairing, and the central TGGT base pairs are propeller-twisted. The C3'-*endo* sugar pucker predominates on the 5'-side of the Pt("A" DNA), and C2'-*endo* puckering occurs on the 3' side ("B" DNA). Coordination of Pt destacks the G(6) and G(7) bases, and one amine ligand hydrogen bonds with a terminal oxygen of the G(6) 5'-phosphate group. Hydrogen bonding of this type also occurs in the crystal structure^[8] of *cis*-[Pt(NH₃)₂{d(pGpG)}]. In this dinucleotide structure, and in that of *cis*-[Pt(NH₃)₂{d(CpGpG)}], there is a switch from C2'-*endo* to C3'-*endo* sugar pucker. The NMR solution structure^[9] of the [Pt(NH₃)₂]²⁺ adduct of the octamer DNA duplex d(CCTG*G*TCC)·(GGACCAGG) also shows kinking towards the major groove (ca. 58°) and unwinding (ca. -21°). Intriguingly, chloride ions promote a very slow rearrangement of this intrastrand crosslink to the G(4)-G(9) interstrand crosslink, so relieving the strain associated with the intrastrand crosslink. In contrast, in the NMR solution structure^[10] of the interstrand crosslink in the decamer duplex d(CATAG*CTATG)·(GTATCG*ATAC), [Pt(NH₃)₂]²⁺ is in the minor groove, the helix sense is reversed from right- to left-handed at G(5), C(6) is extruded, and there is a net unwinding of 87° from A(4) to T(7).

[*] Prof. Dr. P. J. Sadler,^[*] Dr. K. J. Barnham
Department of Chemistry, Birkbeck College, University of London
Gordon House, 29 Gordon Square, GB-London WC1H 0PP (UK)

Dr. S. J. Berners-Price
Faculty of Science and Technology, Griffith University
Nathan, Brisbane 4111 (Australia)

Dr. U. Frey
Institut de Chimie Minerale et Analytique, University of Lausanne
BCH, CH-1015 Lausanne (Switzerland)

[*] Current address: Department of Chemistry, University of Edinburgh
West Mains Road, Edinburgh EH9 3JJ (UK)

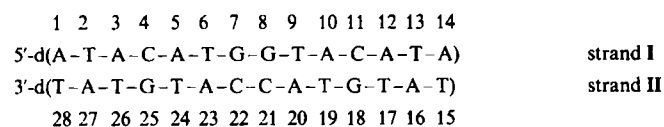
In much of the reported work to date, the duplexes have been prepared by addition of the complementary strand to highly purified platinated GG single strands. Much less is understood about the mechanism of formation of d(GpG) intra- or inter-strand crosslinks on either single strands or duplexes. Such information is important because the lifetimes of the various species along the pathways may determine their biological significance. For example, intermediates may live long enough to be recognized by repair systems, and monofunctional adducts en route to d(GpG) chelates may themselves distort the structure of DNA. Monofunctional binding of $[\text{Pt}(\text{dien})]^{2+}$ is known to lower DNA melting temperatures as much as bifunctional Pt compounds.^[11] Brabec et al.^[12] have shown that the lowerings of the melting temperatures of DNA duplexes (9–20 base pairs) platinated with $[\text{Pt}(\text{dien})]^{2+}$ or $[\text{PtCl}(\text{NH}_3)_2]^+$ are similar, and that monofunctional dG adducts within a pyrimidine–dG–pyrimidine sequence cause a local denaturation such that the C residue on the complementary strand becomes accessible.^[13]

The rate-limiting step in the binding of cisplatin to DNA has long been known to be hydrolysis of the first chloride ion.^[14] A 5'-phosphate group is known to enhance the rate of attack on G residues in mononucleotides,^[15] but in dinucleotides little selectivity of pG over Gp has been observed on platination with $[\text{Pt}(\text{dien})\text{Cl}]^+$ ^[16] or $[\text{Pt}(\text{NH}_3)_3(\text{OH}_2)]^{2+}$.^[17] Elmroth and Lipard have reported that d(GpG) platination of a 16-mer with $\text{cis-}[\text{Pt}(\text{NH}_3)(\text{NH}_2\text{C}_6\text{H}_{11})\text{Cl}(\text{OH}_2)]^+$ occurs around 35 times faster than for a dinucleoside monophosphate.^[18]

Malinge and Leng have reported that monofunctional adducts formed between cisplatin and poly(dG·dC) or *M. luteus* DNA disappear with half-lives of ca. 4 h at 310 K.^[19] Using enriched ^{195}Pt and high concentrations of DNA oligomers (ca. 14–32 mM), Bancroft et al.^[20] have determined that the rate of ring closure of monofunctional intermediates is similar to the rate of chloride hydrolysis.

A significant advance in understanding the kinetics of d(GpG) platination has been made recently by Chottard et al.^[21, 22, 23] who have trapped individual monofunctional adducts during reactions of $\text{cis-}[\text{Pt}(\text{NH}_3)_2(\text{H}_2\text{O})_2]^{2+}$ with single- and double-stranded DNA at pH 4.4. They have found that the 5'-G is platinated faster than 3'-G, but the 3'-G monofunctional adduct chelates faster. The differences were increased in duplexes compared to single strands and were sequence-dependent.

Our own approach to investigating the mechanism of d(GpG) platination involves the observation of ^1H and ^{15}N NMR resonances of Pt– $^{15}\text{NH}_3$ groups.^[24] This allows direct monitoring of reactions of cisplatin with both DNA single strands and duplexes and detection of intermediates at micromolar concentrations. In an initial study^[25] of the platination of the decameric duplex d(ACATGGTACA)·(TGTACCATGT) with cisplatin, kinetic analysis was hampered by the low melting temperature of the duplex, by the apparent formation of three platinated duplexes as final products, and by the formation of interstrand crosslinks by single GG strands at pH 7, probably through GN 7–GN 1.^[26] In the present work we have made a detailed comparison of the kinetics of platination of a related 14-mer duplex (Scheme 1) and its constituent strands using $[\text{H}, \text{N}]$ NMR.



Scheme 1. Structure of 14-mer duplex III.

The increased length of the oligonucleotide has allowed reactions to be studied at a high enough temperature for completion of the reaction to be observed, and a pH of 6 was chosen to avoid interstrand crosslinking of single strands. Since AG sequences are absent, the major product is expected to be the intrastrand GG chelate. The experiments provide the first direct comparison of the kinetics of platination of defined single- and double-strand DNA by cisplatin. A notable finding of potential biological significance is that one of the GG monofunctional adducts of the duplex, but not of the single strand, is very long-lived.

Results

We have used $[\text{H}, \text{N}]$ 2D NMR spectroscopy to study the kinetics of reactions of duplex III with $\text{cis-}[\text{PtCl}_2(\text{NH}_3)_2]$ (1) and $\text{cis-}[\text{PtCl}(\text{H}_2\text{O})(\text{NH}_3)_2]^+$ (2),^[27] and between 1 and the single strands I and II under similar conditions. Normal ^1H NMR spectra were also acquired in particular to investigate base-pairing by detecting the imino resonances at $\delta = 10$ –15 and coordination of N7 of G to Pt by means of H8 resonances. We chose a pH slightly lower than 7 to avoid the complication of coordination to N1 of G during reactions of single strands, and the temperature used (298 K) was a compromise between the need to complete reactions within a reasonable period of time (ca. 60 h) and avoid dissociation of the duplex. Where possible, kinetic analyses of the data were carried out.

Reaction of cisplatin with duplex III: The duplex alone was characterized first. The four GC imino protons gave rise to four peaks between $\delta = 12.3$ and 12.7 at pH 5.96 and 298 K (Fig. 1). The peaks at $\delta = 12.403$ and 12.351 broadened between 313–318 K and can be assigned to the outer GC pairs (base pairs 4 and 11), and the peaks at $\delta = 12.678$ and 12.549 can be assigned to the inner GC pairs since they were still sharp at 318 K. Two sets of peaks at $\delta = 13.427$ and 13.340 are assignable to AT imino protons, and integration of these with respect to the GC peaks indicate that they correspond to 4 protons and 2 protons, respectively. A possible interpretation is that the imino resonances for the outer two AT pairs (A(1)–T(28), T(2)–A(27) and T(13)–A(16), A(14)–T(15); Scheme 1) are too broad to detect and that the $\delta = 13.34$ resonance corresponds to the AT pairs A(3)–T(26) and A(12)–T(17) and the $\delta = 13.43$ peak to pairs at A(5), T(6), T(9) and A(10). The $\delta = 13.34$ peak disappeared between 313 and 318 K and before the $\delta = 13.43$ peak, consistent with the former arising from pairs nearer the ends of the duplex. It was concluded that the melting temperature of the duplex is ca. 318 K and the reactions with cisplatin were subsequently carried out at 298 K.

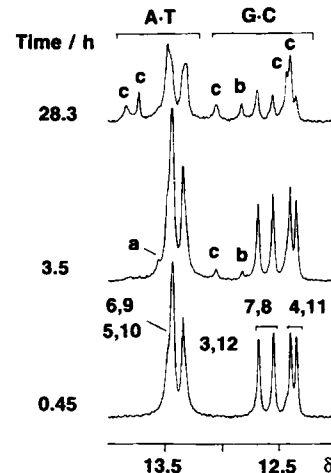


Fig. 1. ^1H NMR spectra (500 MHz) of the imino region of duplex III (1.1 mM, 8.5 mM sodium phosphate, pH 5.96) after 27 min, 3.5 h and 28.3 h of reaction with cisplatin (mol ratio 1:1) at 298 K. Assignments of resonances to base pairs are indicated by numbers (3 = A(3)–T(26), etc.), and letters indicate assignments to platinated duplexes: a 4*, b 3*, c 8*.

The reaction between **III** and [¹⁵N]cisplatin (mol ratio 1:1) at pH 6 in the presence of a small amount of phosphate (9 mM) was followed for a total of 120 h at 298 K. A typical 2D [¹H, ¹⁵N] spectrum obtained after 8 h of reaction is shown in Fig. 2A. All peaks except that for **1** are expected to occur in pairs (two nonequivalent NH₃ ligands in each species), and by following the changes in their volumes with time it was possible to identify the pairs and make assignments based on the expected pathway and on the ¹⁵N shifts which are diagnostic of the *trans* ligand.^[28]

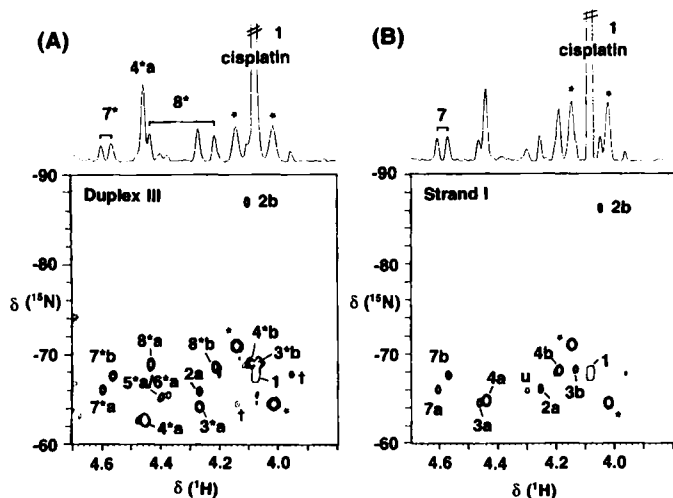


Fig. 2. 2D [¹H, ¹⁵N] HSQC NMR spectra (500 MHz) of: A) Duplex **III** after reaction with [¹⁵N]cisplatin for 8 h. Labels: • ¹⁹⁵Pt satellites, † artefact. Peaks are assigned to NH₃ in structures **1**–**8*** (see Table 1). Peaks **5*a** and **6*a** are tentatively assigned to monofunctional G adducts on the complementary strand (cf. Fig. 6A); partner peaks **5*b** and **6*b** are not resolved but appear at later times. B) Single-strand **I** after reaction with [¹⁵N]cisplatin for 5.3 h. Label: u unknown.

Table 1. ¹H and ¹⁵N NMR chemical shifts, pH 6 (asterisks denote complexes of the duplex).

| Species | $\delta^1\text{H}$ | $\delta^{15}\text{N}$ (<i>trans</i> ligand) |
|--|--------------------|--|
| <i>cis</i> -[PtCl ₂ (NH ₃) ₂] (1) | 4.08 | -67.8 (Cl) |
| <i>cis</i> -[PtCl(H ₂ O)(NH ₃) ₂] ⁺ (2) | 4.25 | -66.1 (Cl) |
| | 4.04 | -86.0 (O) |
| <i>cis</i> -[PtCl(N7G(7))(NH ₃) ₂] (3) | 4.12 | -68.3 (Cl/N) |
| <i>cis</i> -[PtCl(N7G(7))(NH ₃) ₂] (3*) [a] | 4.07 | -69.1 (N/Cl) |
| | 4.27 | -64.1 (Cl/N) |
| <i>cis</i> -[PtCl(N7G(8))(NH ₃) ₂] (4) | 4.18 | -68.0 (N/Cl) |
| | 4.43 | -64.7 (Cl/N) |
| <i>cis</i> -[PtCl(N7G(8))(NH ₃) ₂] (4*) [a] | 4.09 | -69.0 (Cl/N) |
| | 4.46 | -62.7 (N/Cl) |
| <i>cis</i> -[PtCl(N7G(18/25))(NH ₃) ₂] (5/6) | 4.17 | -68.2 (Cl/N) |
| | 4.44 | -65.3 (N/Cl) |
| <i>cis</i> -[PtCl(N7G(18/25))(NH ₃) ₂] (6/5) | 4.13 | -68.2 (Cl/N) |
| | 4.42 | -65.0 (N/Cl) |
| <i>cis</i> -[PtCl(N7G(18/25))(NH ₃) ₂] (5*)/(6*) [b] | 4.13 | -68.2 (Cl/N) |
| | 4.38 | -65.3 (N/Cl) |
| | 4.40 | -65.2 (N/Cl) |
| <i>cis</i> -[Pt(N7G(7)N7G(8))(NH ₃) ₂] (7) | 4.56 | -67.5 (N) |
| | 4.60 | -66.1 (N) |
| <i>cis</i> -[Pt(N7G(7)N7G(8))(NH ₃) ₂] (7*) | 4.57 | -67.5 (N) |
| | 4.60 | -66.0 (N) |
| <i>cis</i> -[Pt(N7G(7)N7G(8))(NH ₃) ₂] (8*) | 4.21 | -68.6 (N) |
| | 4.43 | -68.8 (N) |
| <i>cis</i> -[Pt(H ₂ O)(N7G(7))(NH ₃) ₂] (10*) [c] | 4.50 | -82.8 (O) |
| | 4.36 | -68.7 (N) |
| <i>cis</i> -[Pt(H ₂ O)(N7G(8))(NH ₃) ₂] (11*) [c] | 4.22 | -89.8 (O) |
| | 4.33 | -62.6 (N) |

[a] Tentative assignments based on assumption that 3'-monofunctional adduct ring-closes faster. [b] Group of peaks associated with attack on G residues of complementary strand. [c] Assigned to G(7) and G(8) on the basis of lifetimes in comparison to **3*** and **4***.

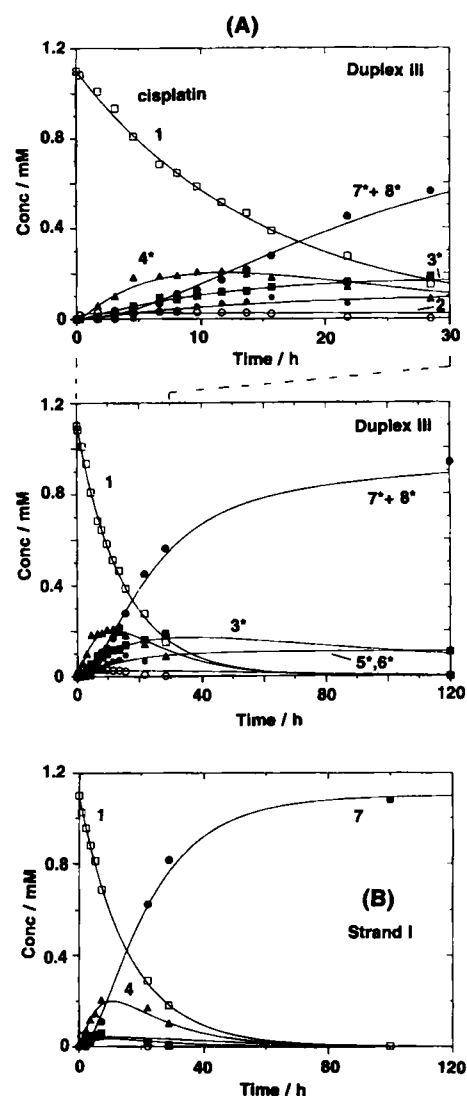


Fig. 3. Plots of relative concentrations of species observed during reactions at 298 K of A) duplex **III** with [¹⁵N]cisplatin. Labels: □ **1**, ○ **2**, ■ **3***, ▲ **4***, ● **5*/6***, ● **7* + 8***. For the purposes of the fit, the sum of the concentrations of the two forms of the GG chelate **7* + 8*** was used. B) Single strand **I** (GG strand) with [¹⁵N]cisplatin. The curves are computer best fits for the rate constants shown in Table 3. Labels: □ **1**, ○ **2**, ■ **3**, ▲ **4**, ● **7**.

The course of reaction is shown in Fig. 3A. It can be seen that the short-lived reactive monoqua hydrolysis product of **1** (complex **2**) is readily detectable even though its concentration is low. Two major intermediates occur, assignable to 3'-G and 5'-G monofunctional adducts (complexes **3***^[29] and **4***), one of which, **3***, is very long-lived and is still present after 120 h of reaction. At least two other minor intermediates (**5*** and **6***) are seen, and these have shifts similar to adducts of the complementary strand **II** with cisplatin (vide infra). These intermediates account for ca. 10% of the total Pt–NH₃, and appeared to be transformed into other products giving peaks at $\delta = 4.42/ -67.1$ and $4.60/ -66.3$ (overlapped by **7***). The latter peaks were also observed during reactions of cisplatin with the complementary strand **II** (see Fig. 6).

The expected final product, the GG chelate, gives rise to two sets of cross-peaks (**7*** and **8***) in each spectrum during the course of reaction. In the early stages (4–12 h) the ratio **8*/7*** increased from 0.6 to 1.7, and from 14 h onwards had a relatively constant value of 2.0–2.5. Peaks for **7*** have shifts very similar to the single-strand GG chelate Pt–I (vide infra). The kinet-

ic fits to the data presented in Figure 3A, gave the rate constants listed in Table 3. One of the G bases in the GG pair is platinated about three times faster than the other, and this same monofunctional adduct disappears to form the GG chelate about thirteen times faster than the other, largely because the latter is very long-lived.

Further evidence for the existence of an equilibrium between **7*** and **8*** as two forms of the GG chelate was obtained from a study on the temperature dependence of the [¹H,¹⁵N] NMR spectrum of the final product of the reaction. As shown in Fig. 4, the proportion of **7*** relative to **8*** increases with temperature, changing abruptly at ca. 306–314 K. At 278 K, over 80% of the chelate is in the form **8***, at 308 K **7*** and **8*** are present in equal amounts, and at higher temperatures **7*** predominates.

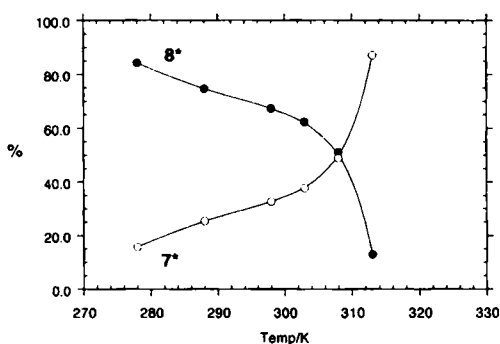


Fig. 4. Dependence on temperature of the relative proportions of complexes **7*** and **8*** GG chelate products from reaction of cisplatin with duplex **III** as determined from the volumes of [¹H,¹⁵N] NMR peaks (see Fig. 2). Studies at temperatures > 313 K were hampered by the overlap of the H₂O peak with the peaks of **7***.

These changes were reversible on lowering the temperature. The temperature dependence of the ¹H NMR spectrum of the final product the GG chelate was also studied. At 278 K there were two singlets at 8.646 and 8.077 assignable^[30] to H 8 protons of G(7) and G(8) of complex **8***. As the temperature increased new peaks at 8.517 and 9.078 (298 K) assignable to **7*** appeared and progressively increased in intensity as those for **8*** decreased in intensity, such that by 323 K only peaks for **7*** were visible. This indicated a melting temperature of ca. 310 K. The broadness of the peaks for **7*** in comparison with those for **8*** suggested that there may be exchange between different structural forms at high temperature. The H 8 shift for **7*** at 298 K is almost identical with that of **7**, the single-strand adduct (Pt–I) (Table 2).

There were several notable changes in the imino region of the ¹H NMR spectrum during the course of the reaction. A new peak appeared at $\delta = 13.558$ in the AT region with a time dependence similar to the [¹H,¹⁵N] peaks for monofunctional adduct **4*** (present in early stages only). In the GC region a new peak at 12.824 had a time dependence similar to **3*** and was still present in the spectrum after 5 d. Two prominent new peaks at low field in the AT region at $\delta = 13.832$ and 13.723 and a peak at $\delta = 13.045$ in the GC region mirror the time dependence of the Pt–NH₃ peaks for the GG chelate **8***. By comparing the relative integrals of the new AT peaks they can be assigned to base pairs 6 and 9, which flank GG, and the new GC imino peak can be assigned to base pair 7 or 8.

Similarly, peaks in the G H 8 region of the ¹H NMR spectrum^[30] were assigned by consideration of their time dependences (Table 2). In the TCH₃ region, the singlet at $\delta = 1.214$ had an identical time profile to the [¹H,¹⁵N] peaks of complex

Table 2. a) ¹H NMR chemical shifts at 298 K for G H 8 protons [a].

| Species | G(8) [3'G] | G(7) [5'G] |
|------------|------------|------------|
| III | 7.763 | 8.240 |
| 3 | | 8.844 |
| 3* | | 8.419 |
| 4 | 8.603 | |
| 4* | 8.033 | |
| 7 | 9.070 | 8.516 |
| 7* | 9.078 | 8.517 |
| 8* | 8.047 | 8.636 |

b) ¹H NMR chemical shifts at 298 K for imino protons.

| | Base pair, δ (AT) | | | Base pair, δ (GC) | | |
|------------|--------------------------|--------|--------|--------------------------|------------|--------|
| | 6/9 | 5/10 | 3/12 | 7/8 | 4/11 | |
| III | 13.427 | 13.427 | 13.340 | 12.678 | 12.549 | 12.403 |
| 4* | 13.558 | | | | | |
| 3* | | | | 12.824 | | |
| 8* | 13.832 | 13.723 | 13.468 | 13.307 | 13.045 [b] | 12.432 |

[a] The assignments for GG chelates are based on known values for other oligonucleotides [30], and for monofunctional adducts, on assumptions about the course of the platination reaction (see footnotes to Table 1). [b] Not resolved.

4* and is shielded by 0.12–0.335 ppm compared to TCH₃ peaks of free duplex. This shielding was not observed for the adducts **3***, **7*** or **8***.

Reaction of cisplatin with single (GG) strand I: The reaction between the single GG strand I and cisplatin was readily followed by [¹H,¹⁵N] NMR spectroscopy. Besides peaks for the chloroaqua complex **2**, two other intermediates **3** and **4** (assignable to monofunctional G adducts) were observable, the latter present in much greater amounts than the former (Figs. 2B and 3B). One other minor unidentified intermediate was present between 4 and 8 h of reaction, but accounted for less than 1% of the Pt–NH₃ present. The reaction was complete within 5 d, and the final product (**7**, the GG chelate) gave two low-field [¹H,¹⁵N] cross-peaks with similar shifts (Table 1). The kinetic fits to the data in Fig. 3B are listed in Table 3, where it can be seen that one of the G residues in the GG is platinated approximately six times faster than the other, although the rates of chelation of the two monofunctional intermediates are similar.

Complex **7** had G H 8 peaks at 8.516 and 9.070 (broad) in the ¹H NMR spectrum. Based on their dependence on time, the peaks at $\delta = 8.603$ and 8.844 observed during the course of the reaction were assigned to H 8 resonances of the intermediates **4** and **3**, respectively.

Reaction of cis-[PtCl(H₂O)(¹⁵NH₃)₂]⁺ with duplex **III:** The reaction between duplex **III** and complex **2** (0.83 molequiv) was followed by [¹H,¹⁵N] NMR spectroscopy at 298 K, pH 6 (Fig. 5). Analyses of the spectra are consistent with the sample of **2** containing ca. 20% diaqua complex and ca. 3% cisplatin as impurities. Peaks assignable to aqua–G complexes **10*** and **11*** (arising from reactions of the diaqua complex with **III**) were present as intermediates up to 1.6 h and 0.3 h, respectively, of reaction time. Although a peak assignable to the aquahydroxo complex^[27] *cis*-[Pt(NH₃)₂(H₂O/OH)]⁺ with the expected shift of $\delta = 4.07 / -86.4$ ^[27] was not observed, a peak at $\delta = 4.58 / -82.4$ was present for up to 4 min and then disappeared. This may be due to an aqua/hydroxo complex associated with the duplex, or perhaps a phosphate or hydroxy-bridged adduct. The initially strong peaks for **2** decreased in intensity over a period of ca. 3 h and gave rise to peaks for two intermediates (**3*** and

Table 3. Rate constants for reactions of duplex III with cisplatin (1) and *cis*-[PtCl(H₂O)(NH₃)₂]⁺ (2), and single strand I with cisplatin at 298 K obtained from computer fits to [¹H,¹⁵N] NMR data. The errors represent one standard deviation. No attempt was made to fit the route from 5*, 6* to other products.

| Rate constant | I + 1 | III + 2 | III + 1 | Diaqua + 8-mer [a] | |
|------------------------------|------------------|-----------------|-----------------|---------------------|----------------------|
| | | | | single strand | duplex |
| Platination | | | | | |
| $k_1/10^{-5} \text{ s}^{-1}$ | 1.73 ± 0.04 | (1.8) [b] | 1.83 ± 0.03 | | |
| $k_2/s^{-1} \text{ M}^{-1}$ | 0.28 ± 0.05 | 0.54 ± 0.02 | 0.47 ± 0.08 | 2.0 | 4.4 |
| $k_3/s^{-1} \text{ M}^{-1}$ | 0.05 ± 0.025 | 0.20 ± 0.01 | 0.15 ± 0.03 | 4.2 | 54 |
| k_2/k_3 | 6 | 3 | 3 | $2 (k_2/k_3)$ | $12 (k_2/k_3)$ |
| Chelation | | | | | |
| $k_4/10^{-5} \text{ s}^{-1}$ | 4.2 ± 0.5 | 4.6 ± 0.3 | 3.2 ± 0.1 | 330 | 80 |
| $k_5/10^{-5} \text{ s}^{-1}$ | 4.5 ± 2.8 | 0.71 ± 0.19 | 0.24 ± 0.18 | 100 | 6 |
| k_4/k_5 [c] | 1 | 7 | 13 | $3 (k_{3c}/k_{5c})$ | $13 (k_{3c}/k_{5c})$ |
| $k_6/s^{-1} \text{ M}^{-1}$ | – | 0.05 ± 0.01 | 0.07 ± 0.01 | – | 40 [d] |

[a] Data from Reeder et al. [23] for d(CTGGCTCA) and d(TTGGCCAA)₂, pH 4.4, 293 K, 0.1 M NaClO₄. [b] Fixed value. [c] k_4 and k_5 may include both hydrolysis and chelation steps; for reactions of the diaqua complex they represent only chelation. [d] Interstrand cross-linking.

4*) in similar proportions and with similar shifts to those observed during reactions of 1 with III (Figs. 2 A and 5 A). Moreover, their dependences on time were also similar (Figs. 3 A and 5 B), with one of them (3*) being very long-lived (still present after 40 h). Peaks attributable to minor adducts with the complementary strand (5* and 6*) reached a maximum intensity after ca. 2 h and accounted for less than 10% of the total Pt–NH₃. These appeared to evolve to products which were not detectable in the final spectrum. As observed during the reaction of cisplatin with III, two GG chelates were again formed: 7* and 8*, although only 7* was seen initially and the ratio of 8*/7* increased from 0.5 at 41 min to 1 after 26 h. Kinetic fits to the data are shown in Figure 5 B, and the kinetic constants are listed in Table 3. As with cisplatin, the faster formed monofunctional G adduct also undergoes the fastest ring closure, and one of the monofunctional intermediates is much longer lived than the other.

Reaction of cisplatin with single (complementary) strand II: [¹H,¹⁵N] NMR cross-peaks for the hydrolysis product 2 of cisplatin were more intense during the reaction of 1.8 mol equiv of cisplatin with the complementary strand II than during the analogous reaction with strand I (Fig. 6). Peaks for two major intermediates appeared with similar shifts and similar time profiles, consistent with these representing monofunctional adducts with G(18) and G(25), complexes 5 and 6 (Table 1). One of the final products gave rise to a pair of sharp cross-peaks at $\delta = 4.43/ -66.7$ and $4.61/ -66.2$ (labelled x in Fig. 6), and other products gave a broad range of peaks between $\delta = 4.3$ to $4.7/ -63$ to -65 . The relative proportions of species observed during the course of reaction are shown in Fig. 6 B. A kinetic fit to these data was not attempted.

In the H8 region of the ¹H NMR spectrum, peaks at $\delta = 8.438$ and 8.497 were assignable to the intermediates 5 and 6 on the basis of their dependence on time, and the broad peaks

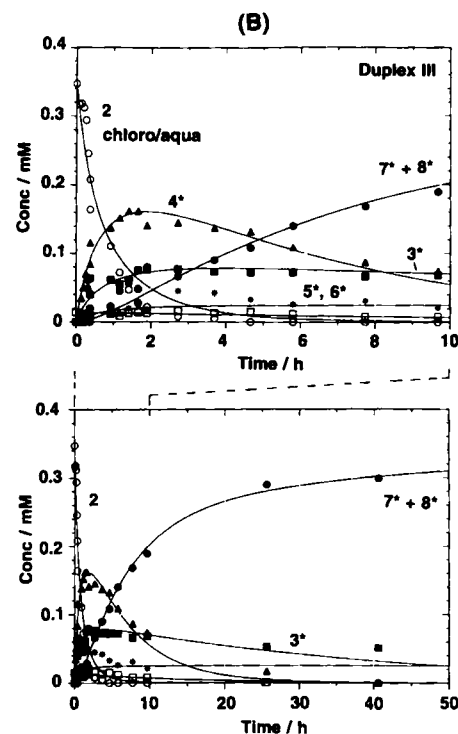
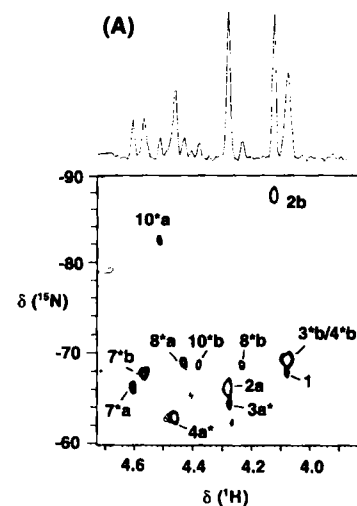


Fig. 5. A) 2D [¹H,¹⁵N] HSQC NMR spectrum (600 MHz) of duplex III (0.56 mM, 9 mM sodium phosphate, pH 5.98) after reaction with *cis*-[PtCl(H₂O)(¹⁵NH₃)₂]⁺ (mol ratio duplex:Pt 1.2:1) for 41 min at 298 K. Peak 10* is assigned to a mono G–aqua complex arising from reaction of diaqua impurity in the sample of 2 with III. The second mono G–aqua complex (11*) is shorter lived. The sample of 2 also contained a small amount of cisplatin 1. B) Plots of relative concentrations of species observed during the above reaction. The curves are the computer best fits for the rate constants shown in Table 3. Labels: □ 1, ○ 2, ■ 3*, ▲ 4*, ● 5*/6*, ● 7* + 8*.

at $\delta = 8.73$, 9.05 and 9.26 appeared after 5 h of reaction time and increased in intensity. The reaction led to a progressive broadening of all ¹H NMR resonances.

Discussion

The kinetic studies of platination of the 14-mer oligonucleotide with cisplatin described here follow on from those we reported previously for a related decamer which lacked the initial AT and final TA bases. Our previous work was carried out at 310 K, pH 7, and although it was possible to follow the initial aquation

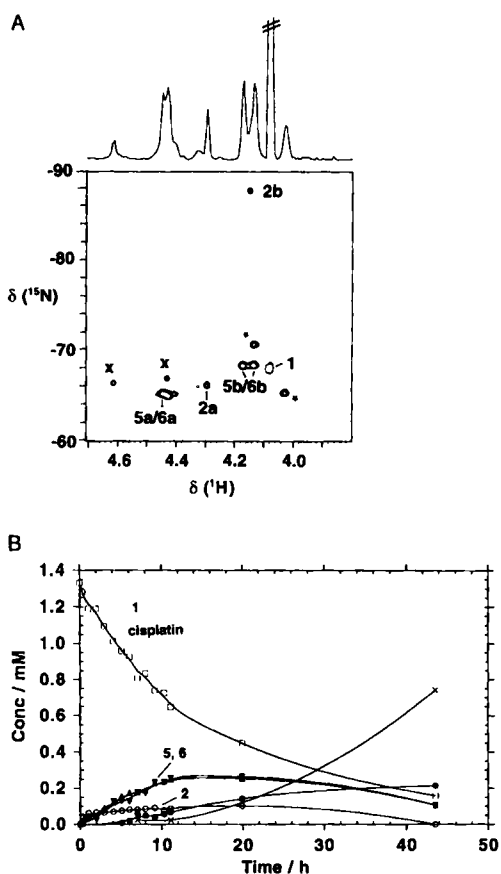


Fig. 6. A) 2D $[^1\text{H}, ^{15}\text{N}]$ HSQC NMR spectrum (600 MHz) of single strand II (complementary strand) after reaction with $[^{15}\text{N}]$ cisplatin for 11.1 h at 298 K. Labels: * ^{15}Pt satellites, x pair of peaks for unidentified final product (possibly interstrand species). B) Plot of relative concentrations of species observed during the above reaction. The smoothed curves are used only to connect the points and clarify the course of reaction. Kinetic fits were not possible under these reaction conditions. Labels: \square 1, \circ 2, \blacksquare 3*, \blacktriangle 5/6, ∇ 6/5, \bullet interstrand, x total other products.

of cisplatin, the formation of two monofunctional adducts (3'-G-Pt and 5'-G-Pt) and the ring closure to give the GG chelate, the reaction of the GG single strand was complicated by the production of possible intermolecular cross-linked species, and the kinetics for the individual monofunctional adducts could not be analysed. Moreover, three products appeared to arise from reactions of the duplex instead of only one expected GG chelate.

In the present study we have carried out reactions at pH 6 to avoid intermolecular reactions of the single strand, and it has been possible to analyse the kinetics of formation and decay of the individual monofunctional adducts. The problem of three products arising from reactions of the duplex was encountered again with the 14-mer and can now be attributed to the existence of a very long-lived monofunctional adduct, which is formed during reactions of the duplex, but not from the GG single strand, together with two forms of the GG chelate. The increased stability of the 14-mer compared to the 10-mer duplex has allowed the kinetics to be followed over a reasonable period of time at 298 K under conditions where the duplex remains intact. This study provides the first direct comparison of platination reactions of defined single and double strands of DNA with cisplatin. As expected, reactions of the duplex with the monoqua complex $\text{cis-}[\text{PtCl}(\text{H}_2\text{O})(\text{NH}_3)_2]^+$ followed the same course as those for cisplatin after the initial hydrolysis step. More than 90% of the platination of the duplex appeared to take place at GG with less than 10% occurring (more slowly) at the isolated G residues on the complementary strands.

The reactions of cisplatin with both the single strand I and the duplex III proceeded via the monoqua hydrolysis product as expected. Two Pt-NH₃ peaks for $\text{cis-}[\text{PtCl}(\text{H}_2\text{O})(\text{NH}_3)_2]^+$ were clearly seen during the early stages of the reactions (Figs. 2 and 3), even though this complex is present at concentrations of less than 50 μM . The rate of hydrolysis determined here is similar to that reported previously.^[31]

Two intermediates (monofunctional adducts) were observed during reactions of the duplex III (3* and 4*) and strand I (3 and 4). The chemical shifts and time-course profiles for 4 and 4* are very similar (Table 1 and Fig. 3), whereas the shifts for one of the Pt-NH₃ ligands in 3* (3*a, Fig. 2) is different from that of 3 (Table 1). This may arise from specific interactions between the Pt ligands and the duplex in 3*, which result in stabilization of the Pt-Cl bond and account for its long lifetime. Since no peaks for aquated monofunctional adducts are seen in the NMR spectra during the course of the reactions of either I or III, it can be concluded that chelate ring closure of both monofunctional adducts is rapid compared to hydrolysis. This is confirmed by the data of Chottard et al.^[23] for reactions of the diaqua complex (Table 3).

The chemical shifts and development with time of peaks attributable to monofunctional adducts of the G residues of the complementary strand II were very similar for both the single strand and duplex (5/6 and 5*/6*, Figs. 2A and 6A; cf. with 3/4 and 3*/4*, Figs. 2A and 2B), perhaps because of end-fraying of the duplex. These monofunctional adducts evolved with time into products that are probably either 1,3-intrastrand or inter-strand crosslinks.

Absolute assignments of 3 or 4 and 3* or 4* to the 3'-G (G(8)) and 5'-G (G(7)) monofunctional adducts cannot be made on the basis of the present data alone. This requires an HPLC separation of the adducts and their identification by chemical and biochemical degradation, which was beyond the scope of the present work. However, it is clear that:

- 1) One of the guanine residues in the GG pair (either the 3'-G or 5'-G) is platinated faster on both the single strand and duplex by a factor of ca. 4 (although it cannot be concluded from our data alone that it is the same G in both single strand and duplex DNA which is platinated faster).
- 2) The monofunctional adduct that forms faster on duplex DNA also ring closes faster to the GG chelate.
- 3) Chelation of one monofunctional adduct on the duplex occurs an order of magnitude faster than the other, whereas there is little difference for the single strand I. This results in a very long-lived monofunctional adduct on the duplex, an adduct of potential biological significance. The chelation rates are of the same order of magnitude as the rate for the first aquation step of cisplatin,^[31] and therefore it can be assumed that the rate of chelation is governed by the second aquation.

Using chicken erythrocyte DNA, Bancroft et al.^[32] determined by ^{195}Pt NMR spectroscopy that the rates of formation of monofunctional and bifunctional adducts on single- and double-stranded DNA at pH 6.5 were approximately the same. The rate constant for closure of monofunctional adducts was similar to that for hydrolysis of the second chloride of cisplatin, and they concluded that chelate ring closure proceeded via the hydrolysed species rather than by direct chloride displacement. They were unable to distinguish between different types of monofunctional adducts. In our case, the rate of GG chelate ring closure of one of the monofunctional adducts is similar to the expected rate of hydrolysis, whereas the other is much slower. However, the actual rates of hydrolysis of monochloro-

monoG DNA adducts are not known. No peaks for the hydrolysed monoadducts were detected during the course of the reaction; so if they are formed, they must be short-lived.

The ratio of chelation rates for the two monofunctional intermediates in reactions of cisplatin and the aquachloro complex would be expected to be the same, whereas values of 13 and 7, respectively, were obtained (Table 3). The difference may reflect the presence of chloride during reactions of cisplatin (released during the first step), which could retard the second hydrolysis and therefore ring closure. However, it should be noted that the errors in the rate constants are relatively high.

In the case of reactions of *cis*-[Pt(NH₃)₂(H₂O)₂]²⁺ at pH 4, it has also been reported^[23] that one of the G residues in a GG pair of d(TTGGCCAA), namely, 5'G, is platinated faster than the other (Table 3), but, in contrast, ring closure is faster for the 3'G monofunctional aqua adduct. Curiously the ratio of the chelation rates for our chloro system and the reported diaqua system is about the same (ca. 13), perhaps because they require similar structural changes in the duplex on formation of transition state complexes during substitution. Indeed peaks assignable to two monofunctional aqua adducts, arising from reactions of diaqua impurity, seen during reactions of **2** with duplex **III** (Fig. 5), also decayed at different rates.

In a GG chelate on a duplex, the greatest steric strain appears to be on the 3'G side.^[9] It can therefore be argued that initial attack on 3'G may lead to a distortion that will more readily allow chelation to 5'G, which is on the more flexible side of the bifunctional lesion. Therefore the long-lived monofunctional adduct may be platinated on 5'G. Significant structural distortions in monofunctional adducts of both duplexes and single strands have been reported. Herman et al.^[33] have reported that in the *cis*-[Pt(NH₃)₂]²⁺ chelate of the decanucleotide duplex d(GCCG*G*ATCGC)·d(CGGCCTAGCG), the C residue complementary to the 5'G is mobile and can stack on either branch of the kinked complementary strand, and in models the sugar of this nucleotide had a general tendency to repucker from S (C2'-endo) to N (C3'-endo). Monofunctional binding of Pt in Pt(dien)[d(AGA)-N7(2)] results in a change in the sugar ring conformation of all three residues from S to 50% N/S,^[34] whereas in Pt(dien)[d(CGT)-N7(2)] only the conformation of the G residue changes upon platination.^[35] ¹H NMR studies have shown^[36] that the formation of the monofunctional adduct [Pt(NH₃)₃]d(TCTCG*TCTC) leads to a change in the sugar pucker of G*(5) from S to 45% N and reduction in dC-dG stacking interactions. The reduction in melting temperature of the corresponding duplex is similar to that for the bifunctional [Pt(NH₃)₂]²⁺ adduct.

We have addressed the problem of the apparent observation of two distinct sets of [¹H, ¹⁵N] NMR peaks (7* and 8*, Fig. 2A) for GG chelate of the 14-mer duplex and have concluded that complex 8* is assignable to a kinked or bent platinated duplex, and that 7* represents distorted forms that have shifts similar to a GG chelate on a single-strand. The changes in imino ¹H NMR resonances for the two AT base pairs flanking the platinated GG of 8*, and the observation of an imino resonance for only one of the (G*G*)·(CC) base pairs is in line with previous reports of a propeller twist of bases around the platination site and more ordering of the duplex at the 3' end compared to the 5' end.^[7, 9] The [¹H, ¹⁵N] chemical shifts of the two Pt-NH₃ groups of 8* are very different (Table 1), unlike those of species 7*, which are similar. This is consistent with differences in the interactions of the two NH₃ ligands of 8* with the duplex. Both the phosphate of 5'-G and C6O of 3'-G^[37] could be involved in H bonding interactions with the coordinated amines. Our data suggest that although 7* has shifts similar to those of the single-strand GG

chelate **7**, it is not a simple single-strand adduct and may be a mixture of distorted conformations depending on the pathway to its formation. For example, during reactions of duplex **III** with the aquachloro complex **2**, more of form 7* of the GG chelate was produced than during reactions with cisplatin.

Forms of 7* may include looped-back structures, partially matched strands and perhaps non-Watson-Crick based-paired forms. Our data suggest that not all forms of 7* are interconvertible with the kinked duplex structure 8*. Elsewhere we will show^[38] that the equilibrium between 7* and 8* can also be detected by CD spectroscopy and can be controlled by pH as well as temperature. Kline et al.^[39] have discussed the melting of d(TCTCG*G*TCTC)·d(GAGACCGAGA) in terms of two sequential structural transitions: duplex melting to give looped-back single strands followed by further disruption at higher temperatures to give single strands.

The distorted form of the platinated decamer duplex d(A-CATG*G*TACA)·(TGTACCATGT) which we studied previously (labelled as species **9** in ref. [25]) did not have the same [¹H, ¹⁵N] NMR shifts as the single-strand GG chelate, and at high temperatures the kinked form of the duplex converted into a mixture of the single-strand form and distorted forms, which gave separate peaks in the [¹H, ¹⁵N] NMR spectrum. In the case of the 14-mer, the single-strand and distorted forms appear to have coincident [¹H, ¹⁵N] Pt-NH₃ chemical shifts.

Although Yang et al.^[9] have reported the rearrangement of the G(4)*G(5)* intrastrand crosslink in d(CCTG*G*TCC)·(GGACCAGG) to an intermolecular G*(4)·G*(9) crosslink, and we have G residues similarly placed in **III**, G(7)·G(18), we observed no spectral changes that can be ascribed to such a rearrangement, and found that the [¹H, ¹⁵N] NMR shifts of **III**-Pt were unchanged even in 0.2M NaCl for 2 d (data not shown). In our case the chloride concentration is 50 times lower, and the rearrangement may only occur if the G residue on the complementary strand is in a very flexible region (e.g., at a frayed end) and can make contact with the G*G* lesion.

Conclusion

By using [¹H, ¹⁵N] NMR spectroscopy it has been possible to compare directly, for the first time, the kinetics of reaction of the anticancer drug cisplatin with defined DNA single and double strands. Reactions with the 14-mer duplex d(A-T-A-C-A-T-G-G-T-A-C-A-T-A)·d(T-A-T-G-T-A-C-C-A-T-G-T-A-T) and the individual strands with [¹⁵N]cisplatin at pH 6, 298 K, proceeded via the aquachloro hydrolysis product **2** of cisplatin, which was readily detectable even though it was present at concentrations of less than 50 μM during the reaction. As expected, reactions of *cis*-[PtCl(H₂O)(NH₃)₂]⁺ itself with the duplex followed similar pathways. The kinetics were analysed in terms of the formation of two monofunctional intermediates in which *cis*-[PtCl(NH₃)₂]⁺ was coordinated to either the 3'-G or 5'-G of the GG pair. The rate of platination of one of the GG residues was faster by a factor of ca. 4 for both the single GG strand and duplex, and the monofunctional adduct that formed faster on the duplex (probably 3'G) also ring-closed faster by about an order of magnitude. One of the monofunctional adducts on the duplex had a surprisingly long lifetime (> 5 d at 298 K), and this adduct had distinct ¹H and ¹⁵N NMR shifts for one of its Pt-NH₃ ligands; this is probably related to the shielding of the Pt-Cl bond from hydrolysis. In contrast, there was little difference between the rates of ring closure of the two monofunctional adducts on the GG single strand. GG platination gave rise to an equilibrium between two major forms of the GG chelate:

a kinked or bent form, and other distorted forms which had [^1H , ^{15}N] characteristics similar to the GG chelate on the single strand.

This study has shown that [^1H , ^{15}N] NMR spectroscopy is a powerful method for investigating the pathways of reaction of platinum anticancer complexes with DNA, and further studies should lead to a better understanding of the factors that govern the reactivity of DNA bases towards platinum. In future work it will be important to investigate the structural basis for the differential reactivity of monofunctional adducts. Such adducts could play an important role in interstrand and DNA-protein cross-linking reactions.

Experimental Procedure

Chemicals: *cis*-[PtCl₂($^{15}\text{NH}_3$)₂] was synthesized as previously described [40] and recrystallized from aqueous KCl. The sodium salts of HPLC-purified oligonucleotides were purchased from OSWEL.

Sample preparation: The courses of reactions at 298 K of **I** and **2** with duplex **III**, and of **1** with single strands **I** and **II** were followed by recording a series of [^1H , ^{15}N] NMR spectra over periods of 40 to 120 h, as appropriate. The samples were prepared as described below.

Reaction of duplex III with cisplatin: To aliquots of strand **I** (40 μL , 0.738 μmol) and strand **II** (40 μL , 0.823 μmol) in H₂O were added D₂O (60 μL), sodium phosphate (30 μL of 200 mM), H₂O (430 μL) and TSP (sodium 3-trimethylsilyl-[D₄]propionate) (1 μL of 20 mM), and the pH was adjusted from 5.2 to 5.96. Then a fresh stock solution of *cis*-[PtCl₂($^{15}\text{NH}_3$)₂] (100 μL of 7.45 mM) was added. The final concentrations were 1.1 mM duplex, 1.1 mM *cis*-[PtCl₂($^{15}\text{NH}_3$)₂], 8.5 mM sodium phosphate, 10% D₂O.

Reaction of single (GG) strand I with cisplatin: An aliquot (40 μL , 0.738 μmol) of a stock solution of strand **I** in H₂O was diluted with D₂O (60 μL), Na phosphate (30 μL , 200 mM in H₂O) and H₂O (470 μL), and the pH adjusted to 6.03. Then aliquots of fresh stock solutions of *cis*-[PtCl₂($^{15}\text{NH}_3$)₂] (100 μL of 7.45 mM) and TSP (2 μL of 20 mM) were added giving final concentrations of 1.05 mM **I**, 1.06 mM *cis*-[PtCl₂($^{15}\text{NH}_3$)₂], 8.5 mM sodium phosphate and 10% D₂O.

Reaction of complementary strand II with cisplatin: An aliquot of a stock solution of **II** (23.6 μL , 0.49 μmol) was diluted with sodium phosphate (30 μL , 200 mM in H₂O), D₂O (65 μL), H₂O (406 μL) and TSP (2 μL , 20 mM), and the pH lowered from ca. 7 to 6.0. Then an aliquot of a solution of *cis*-[PtCl₂($^{15}\text{NH}_3$)₂] in H₂O (125 μL of 7 mM) was added. The final concentrations were 0.75 mM strand **II**, 1.33 mM cisplatin, 9.2 mM Na phosphate, 10% D₂O, pH 6.0 (II:Pt = 1:1.8).

Reaction of duplex III with *cis*-[PtCl(H₂O)($^{15}\text{NH}_3$)₂]⁺: A stock solution of *cis*-[PtCl(H₂O)($^{15}\text{NH}_3$)₂]⁺ was prepared as follows. *cis*-[PtCl₂($^{15}\text{NH}_3$)₂] (22.1 mg, 73.2 μmol) was treated with AgNO₃ (15.3 mg, 90.1 μmol , 1.2 molequiv) in [D₇]DMF (750 μL) overnight at room temperature. The AgCl was removed by centrifugation, and 190 μL of this solution was diluted with 810 μL of H₂O to give a 18.5 mM stock solution of *cis*-[PtCl(H₂O)($^{15}\text{NH}_3$)₂]⁺ in H₂O containing 19% DMF.

To an aliquot (250 μL , 0.37 μmol) of a solution of **I** in H₂O was added sodium phosphate (30 μL , 200 mM in H₂O), D₂O (65 μL), H₂O (280 μL), TSP (2 μL , 20 mM) and a solution of strand **II** (17.9 μL , 0.37 μmol). The pH was adjusted with HNO₃ to pH 5.98, and then the *cis*-[PtCl(H₂O)($^{15}\text{NH}_3$)₂]⁺ solution (16 μL of 18.5 mM) was added. The final concentrations were 0.56 mM duplex **III**, 0.45 mM *cis*-[PtCl(H₂O)($^{15}\text{NH}_3$)₂]⁺, 9 mM sodium phosphate, 9.8% D₂O with 0.5% DMF present (mol ratio duplex:Pt, 1.2:1).

pH Measurements: These were taken with a Corning 240 pH meter equipped with an Aldrich microcombination electrode calibrated with Aldrich pH buffers at pH 4, 7 and 10. HNO₃ and NaOH were used to adjust the pH.

NMR measurements. 1D ^1H and 2D [^1H , ^{15}N] NMR HSQC spectra were recorded on a Varian UNITYplus-500 or a Varian UNITY-600 spectrometer fitted with pulsed field gradient modules. ^1H NMR spectra are referenced to internal TSP and ^{15}N spectra to 1.5 M NH₄Cl in 1 M HCl (external). The WATERGATE sequence [41] was used for H₂O suppression in 1D spectra. Both 1D ^{15}N -edited ^1H NMR spectra and 1D [^1H , ^{15}N] HSQC spectra (optimized for $^1J(\text{N},\text{H}) = 72$ Hz) were recorded using the sequence of Stonehouse et al. [42]. In this sequence coherence selection and suppression of the H₂O signal are achieved by the use of gradient pulses, and the H₂O magnetization is returned to its equilibrium position (z axis) before the start of data acquisition. The ^{15}N spins were decoupled by irradiating with the GARP-1 sequence at a field strength of 1 KHz during the acquisition time.

Unless otherwise stated all spectra were obtained at 298 K, the samples were maintained at this temperature whilst not in the NMR probe, and exposure to light was avoided [43]. Typically for 1D spectra 128 transients were acquired using a spectral width of ca. 10 KHz, relaxation delay of 1.5 s and free induction decays were transformed with exponential weighting functions equivalent to line-broadenings of 0.2–2 Hz. 2D spectra were typically the result of 4–8 transients, acquisition time of 0.15 s, spectral widths of 4 KHz in f_2 , 1.5–2 KHz in f_1 , 32–64 increments of t_1 giving rise to spectra in 4–16 min. They were processed using Gaussian weighting functions in both dimensions, and zero filling by $\times 2$ in f_1 . The acquisition parameters for 2D spectra were varied by changing the number of transients acquired or the number of f_1 increments to allow spectra to be acquired on a timescale suitable for the reaction observed. Routinely, solvent suppression was achieved with VNMR software using a low-pass digital filter of 100 Hz to subtract the zero-frequency component from the time domain data.

Data analysis: For kinetic analysis of NMR spectra peak volumes were measured using Varian VNMR software and the relative concentrations of Pt-NH₃ calculated at each time point. It was assumed that all cross-peaks possess ^{195}Pt satellites. Only those of cisplatin are seen in our spectra; those for the other peaks are presumably broadened owing to relaxation through chemical shift anisotropy [44]. In a few cases there was severe overlap of peaks (e.g., 3*b and 4*b, Fig. 2A), but each species gave rise to a pair of [^1H , ^{15}N] crosspeaks and at least one of the pair was always in a nonoverlapped position. The appropriate differential equations were integrated numerically, and rate constants determined by a nonlinear optimization procedure using the program SCIENTIST (Version 2.0, MicroMath Inc.). The errors represent one standard deviation. For reactions of duplex **III** with complex **2**, it was assumed that the hydrolysis rate of the cisplatin impurity was the same as observed in reactions of cisplatin alone with **III**, and the contribution to the formation of the GG chelate from the diaqua impurity was subtracted at each time point.

Acknowledgments: This work was supported by the Medical Research Council, the Australian NH & MRC (R. Douglas Wright Award to S. J. B.-P.), the Association for International Cancer Research, the Biotechnology and Biological Sciences Research Council (Biomolecular Science Programme), and the Australian Department of Industry, Science, and Technology. The NMR facilities were provided by the Biomedical NMR Centre, Mill Hill. We thank Dr. T. Frenkiel for assistance with NMR experiments, and members of EC COST group D1-0002-92 for helpful discussions, in particular Professor J.-C. Chottard (Paris) for providing data prior to publication.

Received: March 25, 1996 [F332]

- [1] A. Pullman, C. Zakrzewska, D. Perahia, *Int. J. Quantum Chem.* **1979**, *16*, 395–403; A. Pullman, B. Pullman, *Q. Rev. Biophys.* **1981**, *14*, 289–380.
- [2] I. Saito, M. Takayama, H. Sugiyama, K. Nakatani, A. Tsuchida, M. Yamamoto, *J. Am. Chem. Soc.* **1995**, *117*, 6406–6407.
- [3] P. M. Pil, S. J. Lippard, *Science* **1992**, *256*, 234–237.
- [4] A. M. J. Fichtinger-Schepman, J. L. van der Veer, J. H. J. den Hartog, P. H. M. Lohman, J. Reedijk, *Biochemistry* **1985**, *24*, 707–713.
- [5] J. H. J. den Hartog, C. Altona, J. H. van Boom, G. A. van der Marel, C. A. G. Haasnoot, J. Reedijk, *J. Am. Chem. Soc.* **1984**, *106*, 1528–1530.
- [6] B. van Hemelryck, E. Guittet, G. Chottard, J.-P. Girault, T. Huynh-Dinh, J.-Y. Lallemand, J. Igoien, J.-C. Chottard, *J. Am. Chem. Soc.* **1984**, *106*, 3037–3039.
- [7] P. M. Takahara, A. C. Rosenweig, C. A. Frederick, S. J. Lippard, *Nature* **1995**, *377*, 649–652.
- [8] S. E. Sherman, D. Gibson, A. H. J. Wang, S. J. Lippard, *J. Am. Chem. Soc.* **1988**, *110*, 7368–7381.
- [9] D. Yang, S. S. G. E. van Boom, J. Reedijk, J. H. van Boom, A. H.-J. Wang, *Biochemistry*, **1995**, *34*, 12912–12920.
- [10] H. Huang, L. Zhu, B. R. Reid, G. P. Drobny, P. B. Hopkins, *Science* **1995**, *270*, 1842–1845.
- [11] C. J. van Garderen, H. van den Elst, J. H. van Boom, J. Reedijk, *J. Am. Chem. Soc.* **1989**, *111*, 4123–4125.
- [12] V. Brabec, J. Reedijk, M. Leng, *Biochemistry* **1992**, *31*, 12397–12402.
- [13] V. Brabec, V. Boudny, Z. Balcarova, *Biochemistry* **1994**, *33*, 1316–1322.
- [14] N. P. Johnson, J. D. Hoeschele, R. O. Rahn, *Chem.-Biol. Interactions* **1980**, *30*, 151–169.
- [15] M. Green, M. Garner, D. M. Orton, *Transition Met. Chem.* **1992**, *17*, 164–176.
- [16] J. L. van der Veer, H. P. J. M. Noteborn, H. van den Elst, J. Reedijk, *Inorg. Chim. Acta* **1987**, *131*, 221–224.
- [17] A. Laoui, J. Kozelka, J.-C. Chottard, *Inorg. Chem.* **1988**, *27*, 2751–2753.
- [18] S. K. C. Elmroth, S. J. Lippard, *J. Am. Chem. Soc.* **1994**, *116*, 3633–3634.
- [19] J.-M. Malinge, M. Leng, *Nucl. Acids Res.* **1988**, *16*, 7663–7672.
- [20] D. P. Bancroft, C. A. Lepre, S. J. Lippard, *J. Am. Chem. Soc.* **1990**, *112*, 6860–6871.
- [21] F. Gonnet, J. Kozelka, J.-C. Chottard, *Angew. Chem. Int. Ed.* **1992**, *31*, 1483–1485.
- [22] F. Reeder, F. Gonnet, J. Kozelka, J.-C. Chottard, *7th International Symposium on Platinum and other Metal Coordination Compounds in Cancer Chemotherapy*, Amsterdam, **1995**, Abs. 038.
- [23] F. Reeder, F. Gonnet, J. Kozelka, J.-C. Chottard, *J. Inorg. Biochem.* **1995**, *59*, 155; *Chem. Eur. J.* **1996**, *2*, 1068–1076.

- [24] S. J. Berners-Price, U. Frey, J. D. Ranford, P. J. Sadler, *J. Am. Chem. Soc.* **1993**, *115*, 8649–8659.
- [25] K. J. Barnham, S. J. Berners-Price, T. A. Frenkiel, U. Frey, P. J. Sadler, *Angew. Chemie Int. Ed.*, **1995**, *34*, 1874–1877.
- [26] The pK_a of 9-ethylguanine(Hegua) N1 is lowered from 9.57 to 8.02 on platination of N7 with $[Pt(NH_3)_2(Hegua)]^{2+}$: G. Schröder, B. Lippert, M. Sabat, C. J. L. Lock, R. Faggiani, B. Song, H. Sigel, *J. Chem. Soc. Dalton Trans.* **1995**, 3767–3775.
- [27] The pK_a of the aqua ligand in $[PtCl(H_2O)(NH_3)_2]^+$ (**2**) is 6.41: S. J. Berners-Price, T. A. Frenkiel, U. Frey, J. D. Ranford, P. J. Sadler, *J. Chem. Soc. Chem. Commun.* **1992**, 789–791. Therefore, it is largely protonated in the experiments described here.
- [28] T. G. Appleton, J. R. Hall, S. F. Ralph, *Inorg. Chem.* **1985**, *24*, 4685–4693. X-Pt-NH₃; X = O, $\delta = -95$ to -75 ; X = N or Cl $\delta = -70$ to -50 .
- [29] Asterisks in **3***, **4*** etc. denote adducts of duplexes.
- [30] J. Kozelka, M.-H. Fouchet, J.-C. Chottard, *Eur. J. Biochem.* **1992**, *205*, 895–906.
- [31] Rate constants for hydrolysis of cisplatin at 298 K; first step: $2.8 \times 10^{-5} \text{ s}^{-1}$, S. E. Millar, D. A. House, *Inorg. Chim. Acta* **1989**, *166*, 131–137; second step: $2.39 \times 10^{-5} \text{ s}^{-1}$, *ibid.* **1991**, *187*, 125–132.
- [32] D. P. Bancroft, C. A. Lepre, S. J. Lippard, *J. Am. Chem. Soc.* **1990**, *112*, 6860–6871.
- [33] F. Herman, J. Kozelka, V. Stoven, E. Guittet, J.-P. Girault, T. Huynh-Dinh, J. Igolen, J.-Y. Lallemand, J.-C. Chottard, *Eur. J. Biochem.* **1990**, *194*, 119–133.
- [34] G. Admiraal, M. Alink, C. Altona, F. J. Dijt, C. J. van Garderen, R. A. G. de Graaff, J. Reedijk, *J. Am. Chem. Soc.* **1992**, *114*, 930–938.
- [35] C. J. van Garderen, C. Altona, J. Reedijk, *Eur. J. Biochem.* **1988**, *178*, 115–121.
- [36] C. J. van Garderen, C. Altona, J. Reedijk, *Inorg. Chem.* **1990**, *29*, 1481–1487.
- [37] T. W. Hambley, *Inorg. Chem.* **1991**, *30*, 937–942.
- [38] S. J. Berners-Price, A. Corazza, Z. Guo, K. J. Barnham, P. J. Sadler, M. Leng, D. Locker, submitted.
- [39] T. P. Kline, L. G. Marzilli, D. Live, G. Zou, *J. Am. Chem. Soc.* **1989**, *111*, 7057–7068.
- [40] S. J. S. Kerrison, P. J. Sadler, *J. Chem. Commun.* **1977**, 861–864.
- [41] M. Piotto, V. Saudek, V. Sklenar, *J. Biomol. NMR* **1992**, *2*, 661–665.
- [42] J. Stonehouse, G. L. Shaw, J. Keeler, E. D. Laue, *J. Magn. Reson. Ser. A* **1994**, *107*, 174–184.
- [43] D. Payet, M. Leng, *Metal-Based Drugs* **1995**, *2*, 137–141.
- [44] I. M. Ismail, S. J. S. Kerrison and P. J. Sadler, *Polyhedron* **1982**, *1*, 57–9.